

Preparation and characterization of NiO nanorods by thermal decomposition of NiC₂O₄ precursor

CONGKANG XU, GUODING XU, GUANGHOU WANG*

*National Laboratory of Solid State Microstructure and Department of Physics,
Nanjing University, Nanjing 210093, Peoples' Republic of China
E-mail: wangqun@nju.edu.cn.*

Synthesis of nickel oxide (NiO) nanorods was achieved by thermal decomposition of the precursor of NiC₂O₄ obtained via chemical reaction between Ni(CH₃COO)₂ · 2H₂O and H₂C₂O₄ · 2H₂O in the presence of surfactant nonyl phenyl ether (9)/(5) (NP-9/5) and NaCl flux. Transmission electron microscopy (TEM), X-ray diffraction (XRD), Raman spectroscopy, X-ray photoelectron spectroscopy (XPS), selected area electron diffraction (SAED) and high-resolution transmission electron microscopy (HRTEM) were used to characterize the structure features and chemical compositions of the as-made nanorods. The results showed that the as-prepared nanorods is composed of NiO with diameter of 10–80 nm, and lengths ranging from 1 to 3 micrometers. The mechanism of formation of NiO nanorods is also discussed. © 2002 Kluwer Academic Publishers

1. Introduction

One-dimensional (1D) quantum wires or rods are expected to play a vital role as both interconnects and functional components in future mesoscopic electronic and optical devices, and to provide an opportunity to test fundamental quantum concepts. For that reason many preparations of quasi 1D solid nanostructures have been developed, for example, the vapor-liquid-solid (VLS) growth [1–11], solution-liquid-solid (SLS) method [12], template-mediated growth method [13–15], electron-beam lithography (EBL) [16] and scanning tunneling microscopy (STM) techniques [17], and other methods [14–18]. Exploration of novel methods for the large-scale synthesis of 1D nanostructures is a challenging research area. As P-type metal oxide semiconductive materials with a complex band structure, nickel oxide NiO, has received a considerable amount of attention over last few years because of many applications it has found in various field, especially, NiO is a prosperous and interesting material extensively used in catalysis [19], battery cathode [20, 21] gas sensors [22], electrochromic films [23, 24], and magnetic material [25, 26]. NiO naturally exists as mineral bunsenites with a cubic rock salt (NaCl-type) structure. Moreover nanocrystalline NiO is expected to possess many better properties than those of micrometer-sized NiO particles. It is well known that the powder characteristics (particle size, particle size distribution, and shape) are strongly influenced by the preparation process. Nickel oxide is available in two different forms: green or black. The method of the preparation, and especially the temperature, has a profound influence on the properties of NiO [27]. A few methods for the prepara-

tion of nanocrystalline NiO powder have been reported [28–30]. However, up to now, many methods have been developed to synthesize NiO nanoparticles and films, few attempts have been made to prepare NiO nanorods. In this work, we report a simple and novel approach to the fabrication of NiO nanorods by calcining the precursor of NiC₂O₄ obtained via chemical reaction between Ni(CH₃COO)₂ · 2H₂O and H₂C₂O₄ · 2H₂O in the presence of surfactant nonyl phenyl ether (9)/(5) (NP-9/5) and NaCl flux.

2. Experimental procedure

Starting materials are nickel acetate Ni(CH₃COO)₂ · 2H₂O, oxalic acid H₂C₂O₄ · 2H₂O, nonyl phenyl ether (9)/(5)(NP-9/5), and NaCl. Among them, Ni(CH₃COO)₂ · 2H₂O, H₂C₂O₄ · 2H₂O, and NaCl are of analytical grade, NP9/5 is up to 99.0%. 4.98 g of Ni(CH₃COO)₂ · 2H₂O and 2.53 g of H₂C₂O₄ · 2H₂O according to 1 : 1 molar rate were mixed with 5 ml of NP9/5 in a mortar, ground for several minutes and kept in a thermostat oven at 50–60°C for 6 h to prepare the precursor, the product was washed several times with distilled water and acetone to remove remaining reactants, NP9/5 and by-product, and then dried in an oven at 70–80°C for 12 h. The obtained product was collected for the fabrication of NiO nanorods. 2 g of NiC₂O₄, was simultaneously mixed with 8 g of NaCl powder, and then ground for several minutes. The ground mixture was annealed at 900°C for 2 h in a porcelain crucible that was placed in the middle of the alumina tube; the reaction chamber is of alumina tube with a length of 1500 mm and a diameter of 60 mm. After heat treatment, it was gradually cooled to room temperature

*Author to whom all correspondence should be addressed.

(5°C/min), the as-prepared product was washed with distilled water one time, ethanol three times and then ethyl ether one time using an ultrasonic bath and a centrifuge.

The as-prepared product was identified by X-ray powder diffraction (XRD) employing a scanning rate of 0.02 degree/s in a 2θ range from 30° to 100°, using a Japanese Rigaku D/max- γ A X-ray diffractometer equipped with graphite monochromatized Cu K_{α} radiation. The morphologies and dimensions of the products were observed by transmission electron microscopy (TEM), using a JEOL-2010 transmission electron microscope using an accelerating voltage of 200 kV. Meanwhile, the as-made products were also characterized by X-ray photoelectron spectroscopy (XPS), which was carried out on an ESCALAB M K_{II} X-ray photoelectron spectrometer, using Mg- K_{α} X-ray as the excitation source; Raman spectroscopy was obtained using a RFS 100 spectrometer from 0 to 1600 cm^{-1} at room temperature. The 1064 nm line of the laser was used as the excitation source, with the capability of supplying 200 mW. For HRTEM and TEM observation, the as-prepared product was ground in a mortar and suspended in ethanol using an ultrasonic bath for half an hour. A drop was then placed on a holey-carbon copper grid.

3. Results and discussion

The general TEM morphologies of the as-synthesized product are shown in Fig. 1. It can be seen that the product mainly consists of solid rod-like structures. The length of the rods, as shown in Fig. 1a, can be up to several micrometers. The typical nanorod, as can be seen in Fig. 1b, are around 50 nm.

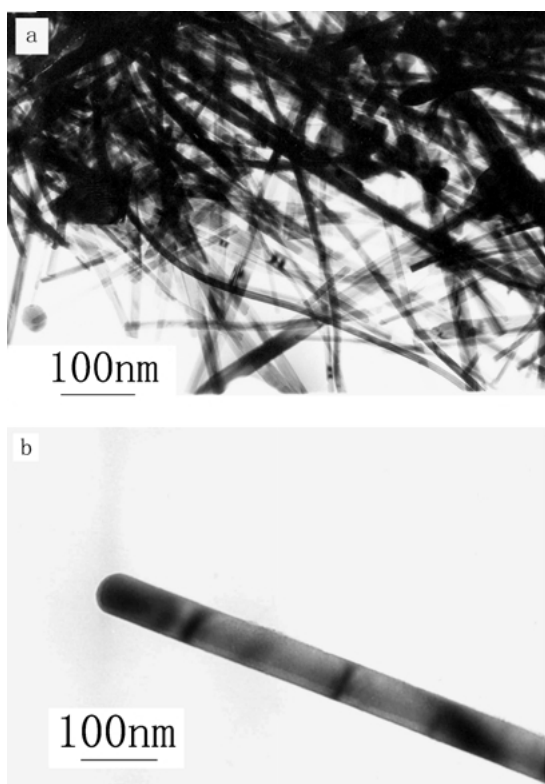


Figure 1 TEM image of the as-prepared NiO nanorods. (a) Morphologies of the as-prepared NiO nanorods. (b) Morphologies of the as-prepared single NiO nanorod.

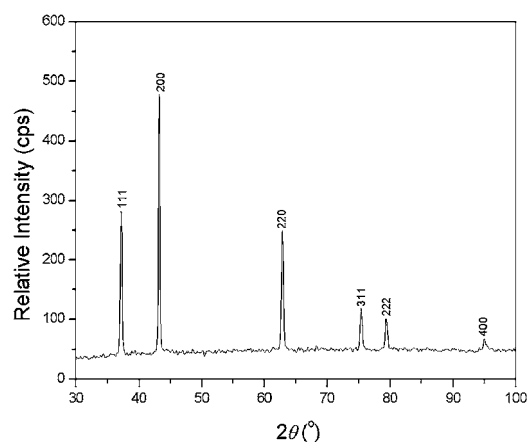


Figure 2 The XRD pattern of the as-prepared NiO nanorods.

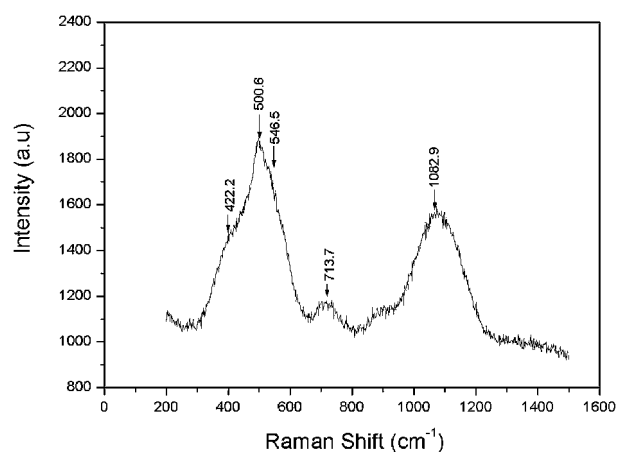


Figure 3 The Raman spectra of the as-prepared NiO nanorods.

Fig. 2 shows the XRD of the as-prepared products obtained by thermal decomposition of the precursor of NiC_2O_4 .

The reaction is as follows:



Its diffraction peaks were quite similar to those of a bulk NiO, which can be indexed as the bunsenite structure NiO and diffraction data were in agreement with JCPDS card of NiO (JCPDS 4-0835). No characteristic peaks of impurities such as NaCl and NiC_2O_4 were observed. Thus, the results showed that the as-prepared product is single-phase bunsenite structure NiO.

Fig. 3 shows the Raman spectra of the as-made NiO nanorods. It can be seen that there are five Raman peaks at 422.2, 500.6, 546.5, 713.7 and 1082.9 cm^{-1} , respectively. Compared with the predicated data of the cubic NiO single crystal [31], the peaks at 422.2 and 546.5 cm^{-1} can be assigned to first order transverse optical (TO) and longitudinal optical (LO) phonon modes of NiO. The peaks at 713.7 and 1082.9 cm^{-1} can be assigned as combination of 2TO and 2LO, which are all shifted down in frequency about 65 cm^{-1} . The remaining peak at 500.6 cm^{-1} is supposed to superimposition of 422.2 and 546.5 cm^{-1} . For $k=0$ phonons in the paramagnetic phase transform as Γ_4^- , no first order

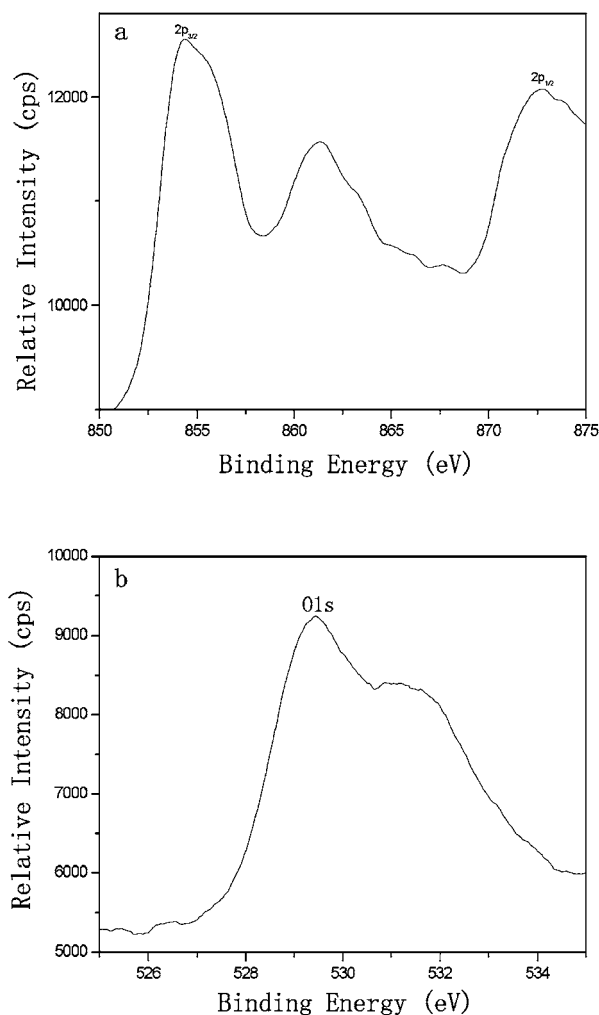


Figure 4 The XPS analysis of the as-prepared NiO nanorods. (a) Ni region. (b) O region.

Raman scattering is expected. Therefore the observed first order Raman peaks near 422.2 cm^{-1} (TO) and 546.5 cm^{-1} (LO) must derive from parity breaking imperfections. This conclusion is confirmed by the enhancement of the first order Raman scattering in the black NiO, where the nickel vacancy concentration is high.

Fig. 4a and b show XPS spectra taken from the Ni and O regions of the sample. The peaks at about 872.6 eV and 853.6 eV are attributed to $Ni2p_{1/2}$ and $Ni2p_{3/2}$ (Fig. 4a), respectively, which are close to the data for Ni (2p) in NiO, the peak at 853.6 eV has a shake-up satellite at about 7.7 eV higher in binding energy than that of the main peak. The gap between the $Ni2p_{1/2}$ and $Ni2p_{3/2}$ level is 19 eV that is approximately the same as in the standard spectrum of Ni; the peak at 853.6 eV is assigned to the Ni^{2+} state in NiO. From Fig. 4b, it is seen that the O_{1s} XPS is asymmetric, indicating that at least two oxygen species are present in the nearby region. The peak at about 530 eV is due to oxygen in the NiO crystal lattice, whereas the peak at about 532 eV is due to chemisorbed oxygen caused by surface hydroxyl. Peak area of the Ni (2p) and O (1s) cores were measured and used to calculate the chemical composition of the sample. Areas were determined by fitting each of the curves using a nonlinear least squares curve fitting program, and taking the area of the fitting peak.

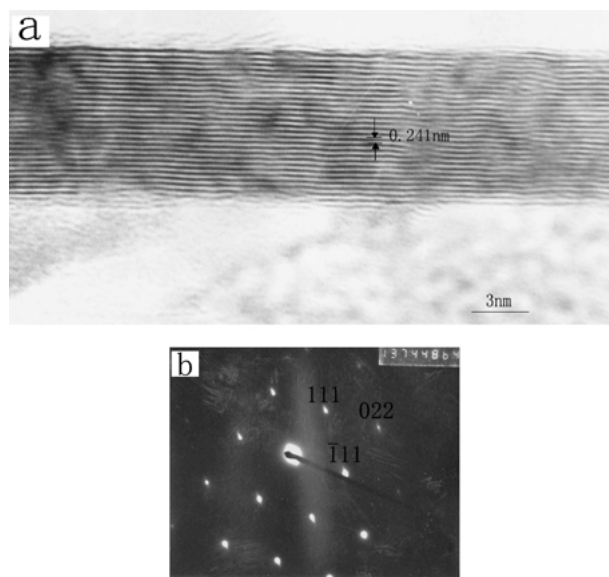


Figure 5 HRTEM micrograph and SAED of one single crystalline NiO nanorods. (a) HRTEM micrograph of a 50 nm NiO nanorod. (b) SAED of a 50 nm NiO nanorod.

The quantification of the peaks gives the atomic ration of Ni : O is nearly 1 : 1. Thus the XPS results clearly proved that the sample is composed of NiO.

The atomic structure detail of the nanorods was revealed using HRTEM. Fig. 5a is an HRTEM image of a representative nanorod with diameter of about 50 nm. The selected-area electron diffraction (SAED) patterns (Fig. 5b), taken from the same nanorod shown in Fig. 1b, can be indexed to the reflection of cubic rock salt NiO structure with lattice parameters of $a = 4.1769\text{ \AA}$, which is in consistent with the above XRD results. HRTEM image shows that the nanorods is nearly structurally uniform, and the clear lattice fringes illustrate that the nanorod is a single crystalline. The interplanar spacing (Fig. 5a) is about 0.241 nm, which corresponds to the [111] plane of cubic crystalline NiO, indicating that the growth plane on the nanorods is along the [111] planes.

In addition, the generalization of this approach must require insight into the formation mechanism of nanorods. There usually exist two models that explain the mechanism of growth for nanorods [18]. One is the VLS growth mechanism; the other is the conventional spiral mechanism. In our product, there is no evidence that the NiO nanorod growth matches the former. There are no droplets observed on any end of the nanorods, which is the most remarkable sign of the VLS mechanism. There exists a conical tip at the end of nanorod (Fig. 1b), which is evidence of the spiral growth mechanism.

Obviously, the formation of the nanorods must be affected by the character of the starting material, such as, the particle size and/or chemical activity in that the dissolution rate of the material depend upon these characters. The viscosity of the flux during calcination and the eutectic temperature of the system also affect the formation of the nanorods. We found that the NiO nanorods fail to form in the absence of NaCl and surfactant NP-9/5 or either of them. Only in this way can the

NiO nanorods be formed in the presence of the suitable NaCl and surfactant NP-9/5. We speculated that NaCl may significantly decrease the viscosity of the melt, and make mobility of components in the flux become easier, i.e., provide a favorable environment for the growth of nanorods, the surfactant NP-9/5 is favorable to form fine particle and make a "shell" surrounding the particles to prevent them from aggregating to larger particles during the grinding process of the precursor, on the other hand, during the formation of NiO nanorods, surfactant was thought to be able to act a template, with the template action resulting in the epitaxial growth of the product. It is interesting to note that the precursor takes the shape of rod-like structure if the surfactant NP9/5 is sufficient. A detailed study of mechanism of NiO nanorods is in progress.

4. Conclusions

In summary, NiO nanorods with diameters of 10–80 nm and lengths of several micrometers have been successfully prepared by a simple and novel method. The as-prepared NiO nanorods are structurally uniform, single crystalline. The growth mechanism of the NiO nanorods is most likely controlled by the VS growth mechanism. Particularly, surfactant NP-9/5 is of critically importance for the formation of NiO nanorods. If properly choosing surfactant, this method may be extended to other metal oxide nanorods.

Acknowledgments

This work was financially supported by the National Nature Science Foundation of China (No.29890210, 10023001, 10074024).

References

1. A. M. MORALES and C. M. LIEBER, *Science* **279** (1998) 208.
2. D. P. YU, C. S. LEE, I. BELLO, X. S. SUN, Y. H. TANG, G. W. ZHOU, Z. G. BAI, Z. ZHANG, S. Q. FENG and D. P. YU, *Solid State Commun.* **105** (1998) 405.
3. G. W. ZHOU, Z. ZHANG, Z. G. BAI, S. Q. FENG and D. P. YU, *Appl. Phys. Lett.* **73** (1998) 677.
4. D. P. YU, Z. G. BAI, Y. DING, Q. L. HANG, H. Z. ZHANG, J. J. WANG, Y. H. ZOU, W. QIAN, G. C. XIONG, H. T. ZHOU and S. Q. FENG, *ibid.* **72** (1998) 3458.
5. H. Z. ZHANG, D. P. YU, Y. DING, Z. G. BAI, Q. L. HANG and S. Q. FENG, *ibid.* **73** (1998) 3396.
6. J. WESTWATER, D. P. GOSAIN, S. TOMIYA, S. U. SUI and H. RUDA, *J Vac. Sci. Technol. B* **15** (1997) 554.
7. D. P. YU, Q. L. HANG, Y. DING, H. Z. ZHANG, Z. G. BAI, J. J. WANG, Y. H. ZHOU, W. QIAN, G. C. XIONG and S. Q. FENG, *Appl. Phys. Lett.* **73** (1998) 3076.
8. Y. Q. ZHU, W. B. HU, W. K. HSU, M. TERRONES, N. GROBERT, T. KARALI, H. TERRONES, J. P. HARE, P. D. TOWNSEND, H. W. KROTO and D. R. M. WALTON, *Adv. Mater.* **11** (1999) 844.
9. K. HIRUMA, M. YAZAWA, T. KATSUYAMA, K. OGAWA, K. HARAGUCHI, M. KOGUCHI and H. KAKIBAYASHI, *J. Appl. Phys.* **77** (1995) 447.
10. G. W. MENG, L. D. ZHANG, Y. QIN, F. PHILLIPP, S. R. QIAO, H. M. GUO and S. Y. ZHANG, *Chin. Phys. Lett.* **9** (1998) 689.
11. X. T. ZHOU, N. WANG, H. L. LAI, H. Y. PENG, I. BELLO, N. B. WONG and C. S. LEE, *Appl. Phys. Lett.* **74** (1999) 3942.
12. T. J. TRENTLER, K. M. HICKMAN, S. C. GEOL, A. M. VIANO, P. C. GIBBONS and W. E. BUHRO, *Science* **270** (1999) 1791.
13. H. DAI, E. W. WONG, Y. Z. YU, S. S. FAN and C. M. LIEBER, *Nature* **375** (1999) 769.
14. W. Q. HAN, S. S. FAN, Q. Q. LI and Y. D. HU, *Science* **277** (1997) 1287.
15. W. Q. HAN, S. S. FAN, Q. Q. LI and B. L. GU, *Appl. Phys. Lett.* **71** (1997) 2271.
16. E. LEOBANDUNG, L. GUO, Y. WANG and S. Y. CHOU, *ibid.* **67** (1997) 938.
17. T. ONE, H. SAITOH and M. ESASHI, *ibid.* **70** (1997) 1852.
18. H. Z. ZHANG, Y. C. KONG, Y. Z. WANG, X. DU, Z. G. BAI, J. J. WANG, D. P. YU, Y. DING, Q. L. HANG and S. Q. FENG, *Solid State Commun.* **109** (1999) 677.
19. D. LEVIN and J. Y. YING, *Stud. Surf. Sci. Catal.* **110** (1997) 367.
20. M. YOSHIO, Y. TODOROV, K. YAMATO, H. NOGUCHI, J. ITOH, M. OKADA and T. MOURI, *J. Power Sources* **74**(1) (1998) 46.
21. H. X. YANG, Q. F. DONG, X. H. HU, X. P. AI and S. X. LI, *ibid.* **79**(2) (1999) 256.
22. TAKENOSHITA and HIDEHIRO, Patent JP 09263444 7,10, 1997, p. 6.
23. E. L. MILLER and R. E. ROCHELEAU, *J. Electrochem. Soc.* **144**(9) (1997) 3072.
24. Y. WU, G. WU and X. NI, *J. Vac. Sci. Technol.* **19**(3) (1999) 228.
25. Y. WANG and J. KE, *High Technol. Lett.* **3**(1) (1997) 92.
26. A. C. FELIC, F. LAMA and M. J. PIACENTINI, *Appl. Phys.* **80**(12) (1997) 3678.
27. Ullmann's Encyclopedia of industrial Chemistry, Vol. A17, 238 (1991).
28. J. L. SHI, J. H. GAO and Z. X. LIN, *Solid State Ionics* **32** (1989) 537.
29. A. CHATTERZEE and D. J. CHAKRAVOTY, *J. Mater. Sci.* **27** (1992) 4115.
30. Y. WANG and J. J. KE, *Mater. Res. Bull.* **31**(1) (1996) 55.
31. R. E. DIETZ, G. I. PARISOT and A. E. MEIXER, *Phys. Rev. B* **4** (1971) 2302.

Received 30 January
and accepted 9 August 2002